

CORRELATION OF AIR-PERMEABILITY AND SLAG CORROSION RESISTANCE OF ADVANCED CARBON-CONTAINING REFRACTORY MATERIALS FOR HIGH-TEMPERATURE APPLICATIONS

Goutam Ghosh*, Rinu Pradhan, Biswajit Sahu, Monoj Halder, Prasanta Panigrahi
TATA STEEL, TATANAGAR, India

*goutam.ghosh2@tatasteel.com; Phone no- +91-9263632190

Key Word: Permeability, Corrosion, thermal spalling, carbon-containing refractories

ABSTRACT

There is a steady demand for high-performance advanced carbon containing refractory to cope with increasing steel production. For accurate prediction of refractory performance in plant application, estimating the effect of corrosion by metal or slag on refractory is essential. Corrosion properties are mainly affected by apparent porosity, permeability, oxidation, and thermal spalling resistance. Air permeability has a substantial effect on the slag corrosion resistance of the materials. Magnesia carbon refractory materials with low, medium, and high permeability values were performed a finger corrosion test in an induction furnace at application temperature. Microstructural study of the samples was conducted along with thermo-mechanical, thermal spalling, and oxidation properties. This present work aims to achieve the correlation between permeability and slag corrosion resistance, which will bring forth the potential benefits of

optimizing the refractory permeability property for better performance in our plant.

INTRODUCTION

Graphite containing MgO–C refractory is a special type of carbon bonded oxide refractory in steel production with use as working lining for basic oxygen furnace (BOF) and slag zone of the steelmaking ladle steel making process. Magnesia carbon (MgO-C) refractory materials consist of fused magnesia and carbon as a base raw material. They are formed by the addition of resol resin to create a carbon network inside the matrix. These refractory materials offer excellent thermo-mechanical properties, thermal spalling resistance, and good corrosion resistance under service at elevated temperatures. These good characteristics are achieved by the addition of graphite attributed to its high thermal conductivity and low thermal expansion coefficient, and non – wetting nature. However, poor oxidation resistance of

This UNITECR 2022 paper is an open access article under the terms of the [Creative Commons Attribution License, CC-BY 4.0](#), which permits use, distribution, and reproduction in any medium, provided the original work is properly cited.

graphite can oxidize in air to form both CO and CO₂ gases, leading to an increase in porosity of the refractory, corrosion, and poor hot strength [1-3].

Further, adding more significant amounts of graphite to the refractory involves several drawbacks reported in detail elsewhere [4]. These key factors lead to the evaluation of low carbon refractories that constitute lesser graphite content. However, the demand of developing low carbon-containing oxide refractories without comprising the beneficial thermomechanical and thermochemical properties is a challenging task that introduces the use of new technology in refractory fabrication [5-6]. These refractories generally have a complex structure consisting of a solid portion of one or more crystal phases, glass, and porous portion. The pores in the refractories are separated into open pores connected to the surface and closed pores isolated inside the brick. The volume of pores inside a brick controls its mechanical and thermal properties and its reaction with various gases and liquids during use at high temperature. Pores included in refractories have a close relationship with the permeation of slag and reaction with gases and significantly influence the attrition of refractories. The open pores and a series of interconnected pores are directly related to the depth and amount of slag penetration.

Permeability indicates the extent of pore linkage in a refractory.

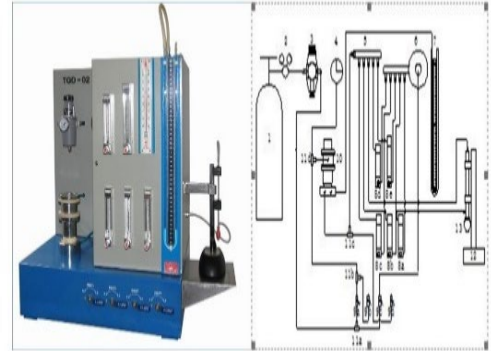


Figure 1 Schematic diagram of permeability apparatus

EXPERIMENTAL PROCEDURE

Three samples of commercial Magnesia Carbon bricks denominated MC1 to MC3 with different permeability values, as mentioned in table 1, were selected to correlate permeability, spalling, and corrosion properties. Permeability test was conducted in permeability apparatus (make: LIRR, China) as shown in Figure 1. Permeability of the samples is conducted in 50 mm diameter and 50 mm height samples. Samples are oxidized at 1000°C for four h in the electrical heated furnace after conducting a permeability test. MC-1 quality has the lowest, and MC-3 has the highest permeability; as shown in Table 1, magnesia carbon bricks are used for the steel ladle slag zone in steel making area. Chemical

analysis of the samples was done using the Inductively coupled plasma mass spectrometry (ICP-MS) method. Both optical (Zeiss) and Scanning Electron Microscopes (SEM-Hitachi operating at 20kV voltage) were employed to observe the microstructure of the samples. Elemental analysis of different phases present in the sample was conducted using SEM coupled with an energy dispersive spectroscopy (EDS) unit. Bulk density (BD) and apparent porosity (AP) were determined by both DIN EN 993-1(DIN51056) standard. Thermal expansion was measured to 1400 degree C at a 5 degree C heating rate to 250 degree C at temperature -falling speed 5 degree C per minute using Dilatometer DIL-402C by Netzsch. Powder samples are tested in air atmosphere up to 1400 degree C temperature with 5 degree C per minute heating rate. A slag corrosion test was conducted in an induction furnace (make: Inductotherm) at 1600 degree C temperature with steel ladle slag.

Table 1 Permeability value of samples

Quality	Permeability value
MC-1	0.47
MC-2	0.55
MC-3	0.7

3 Results

The chemical analysis of the bricks is shown in Table 2. The physical properties of the

materials are analyzed to understand the changed behaviour of the materials, as shown in Table 3.

Table 2: Chemical properties of the bricks

Test element (Weight %)	MC-1	MC-2	MC-3
Al ₂ O ₃	3.70	3.65	3.55
MgO	91.64	91.05	91.28
CaO	1.46	1.20	1.33
Fe ₂ O ₃	1.01	2.09	2.01
SiO ₂	1.51	1.25	1.39
FIXED CARBON(FC)	11.51	11.25	11.33
Loss on Ignition(LOI)	1.14	1.85	1.34
Volatile Matter(VM)	12.65	13.10	12.67

Table 3 Physical properties of sample bricks

Test properties	MC-1	MC-2	MC-3
AP AS RECEIVED (%)	1.98	2.11	2.45
AP COOKING 1000 degree C for 4 h (%)	8.36	8.46	9.11
BULK DENSITY (gm/cc)	3.04	3.05	3.05
BD COOKING AT 1000°C for 4 h (gm/cc)	2.98	2.98	2.98

Cold Crushing Strength (kg/cm ²)	334	340	320
Cold Crushing Strength After firing at 1000 °C for 4 h (kg/cm ²)	240	220	195

Thermal expansion is an essential data point for the design of the refractory structure, and it is a critical parameter that plays a role in thermal shock resistance. A reversible thermal expansion curve was obtained with the help of a push rod dilatometer from room temp to 1400°C. The heating rate was 5°C per minute. Figure 2 shows that there is not much difference in the thermal expansion values of existing and improved quality magnesia carbon bricks. Figure 3 shows the DSC TG graph of the three samples up to 1400 degree C in a 5-degree heating rate in a normal atmosphere.

Table 4 shows the PSD distribution of the samples conducted in a mercury porosimeter machine to understand the distribution of the pores. A good correlation was observed of permeability value along with the permeability value. For a given pore volume, a large size pore will have more area to react with the slag materials compared to a small size

pore. So, higher pore size materials are observed to have more corrosion in the presence of slag.

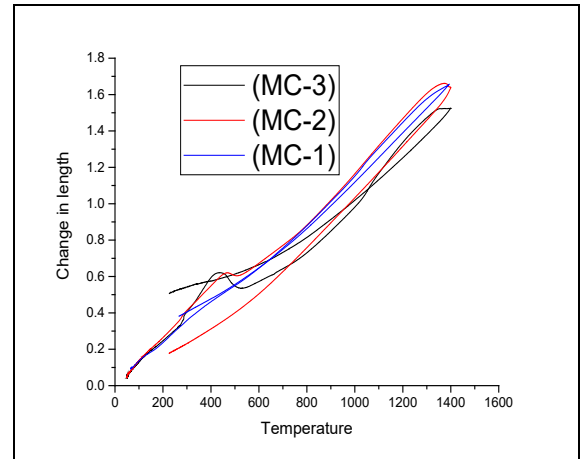


Figure 2 Reversible thermal expansion curve

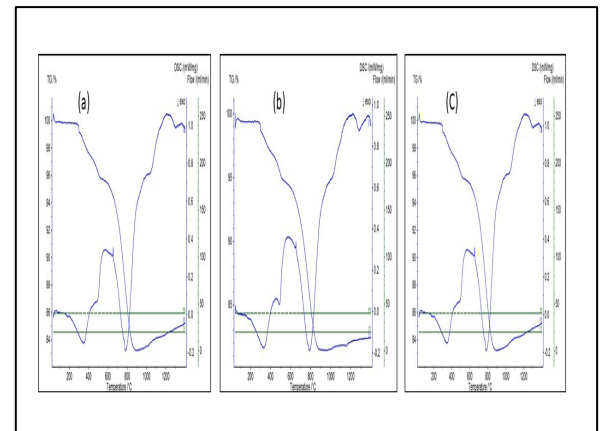


Figure 3 DSC-TG curve: (a) MC-1, (b) MC-2 and (c) MC-3

Table 4 PSD of the magnesia carbon samples

Parameters	MC-1	MC-2	MC-3
Median pore dia. (Vol), micron	6.9317	12.343	35.271
Median pore dia. (Area), micron	0.0265	0.1224	0.4593

Avrg. pore dia. (4V/A), micron	0.4628	2.453	8.119
Pore size distribution (Micron), %			
>100	0.5	3.1	6.1
(60-100)	2.2	11.3	21.4
(40-60)	2.4	12.2	18.4
(20-40)	3.4	20.9	30.6
(10-20)	25.2	16.3	13.8
(5-10)	24.2	12.4	4.2
(1-5)	33.6	9.6	3.1
(0.5-1)	3.2	5.7	2.4
(0.2-0.5)	1.6	1.5	Nil
(0.01-0.2)	3.7	Nil	Nil

Microstructure

SEM provides detailed high-resolution images of the sample by focusing electron beam across the surface and detecting secondary or backscattered electron signals. An Energy Dispersive X-Ray Analyzer provides elemental identification and quantitative compositional information. EDS analysis shows that high purity FM grains are used in MC-2 material along with smaller size antioxidant materials.

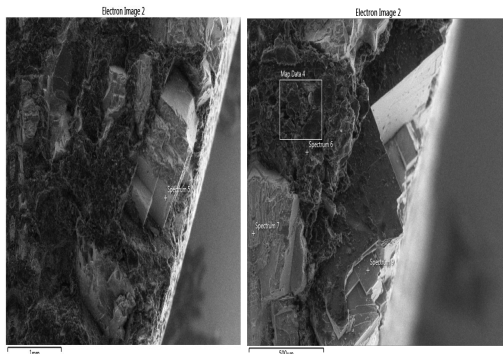


Figure 4 SEM of samples: (a) MC-1, (b) MC-2 and (c) MC-3

Corrosion test

This slag corrosion test was done with steel ladle slag at 1600°C with magnesia carbon bricks with a soaking time of 0.5 hours. The induction furnace dip test was done with a sample size of 40x40x150mm. This arrangement provides slag to flow over the materials at high temperatures. From Fig 5, we can visualize that the MgO-C brick is getting oxidized from the outer surface. Details measurement of corrosion is given in table 4. Corrosion index shows MC-3 have higher corrosion over MC-1 sample.

Table 5 Chemical composition of the slag

Sample	LF slag
Al ₂ O ₃	31.2
MgO	4.5
CaO	55.8
TiO ₂	0.3
Fe ₂ O ₃	2.5
SiO ₂	0.29



Figure 5 Pictures after Corrosion Test

Table 6 Corrosion index of the samples

Quality	Corrosion index
MC-1	3.6
MC-2	5.96
MC-3	10.6

Figure 5 shows the photographs of the corroded sample after the slag corrosion test, where a neck formation corresponds to the penetration depth. Slag penetration was found to be minimum for MC-1 and highest for MC-3 bricks. The corrosion index of the three samples is given in table 4. The corrosion index shows MC-1 has better corrosion properties than the other two samples.

DISCUSSION

As shown in Table 2, chemical results indicate that the magnesia, graphite, and antioxidants percentage are not changed in the three samples. The CaO/SiO₂ ratio of the samples is in close range indicate that the samples are prepared with the same base raw materials as evident from the chemical composition of the bricks. From a chemical purity point of view, all three samples are similar.

In Table 3, the coked apparent porosity of the MC-1 is lower than the other two samples. Apparent porosity refers to open pores in a material. Open-pore increase exposes the higher surface area of the material to the slag.

We observed an increase of porosity of the samples after firing at 1000 degree C in coking condition. Bulk density in as such and coked condition in both samples is similar and indicates similar raw materials.

The reversible expansion is followed in the design of Refractory lining for the provision of expansion joints. The lower thermal expansion of the bricks is less susceptible to spalling. RTE test is carried out on a sample of each type of brick. In figure 3, we observed that MC-3 bricks have a lower thermal expansion value at 1400 degree C, and MC-1 bricks have a higher thermal expansion value.

The corrosion behavior of the sample is like the observation in the permeability test. Lower the permeability value better the corrosion resistance.

CONCLUSIONS

The present investigation regarding the effect of permeability on the corrosion of magnesia carbon bricks revealed the following points:

1. We have found a strong positive influence of air permeability and corrosion index of carbon-containing advanced refractory. A lower permeability value will increase the corrosion resistance of the magnesia carbon materials.
2. The factors that decide permeability of the magnesia carbon refractory

- areas such as coked porosity, microstructure, thermal expansion
3. The lower permeability of the bricks leads to thermal spalling during application. Optimum permeability is essential for the high-temperature solid and gaseous reactions inside the magnesia carbon refractory.
 4. With optimum permeability, we get higher corrosion resistance and thermal spalling resistance which leads to better performance in the steel ladle slag zone in the plant was observed.
5. Yamaguchi, A., Control of oxidation-reduction in MgO-C refractories. *Taikabutsu Overseas*, 1984, 4(1), 332-337
 6. Nobuhiro Maruoka, Akira Ishikawa, Hiroyuki Shibata, and Shin-ya Kitamura, Competitive Dissolution of MgO from Flux and refractory, UNITEC 2011, Vol-3, 1-E-17
 7. Shingo Umeda, Tadashi Ikemoto, and Kiyoshi Goto; Effect of thermal treatment on corrosion resistance of magnesia carbon converter bricks, UNITEC 2011, Vol-3, 1-E-16
 8. Dr. Michel RIGAUD, Advanced seminar on refractories for steelmaking, Mechanism of wear, Page-70, September 25-26, 2007
 9. Xu, Y., Sang, S., Li, Y. et al. Metall, and Mat Trans A (2014) 45: 2885. <https://doi.org/10.1007/s11661-014-2217-1>

REFERENCE

1. E. Mohamed, M. Awais, Carbon-based refractories, *Journal of the Ceramic Society of Japan* 112 (10) (2004) 517–532.
2. Yamaguchi, A., 2003. Features and future development of the carbon-containing refractory. *Key Engineering Materials*, 247(3), pp.239-244.
3. Behera, S. and Sarkar, R., 2016. Nano carbon-containing low carbon magnesia carbon refractory: an overview. *Protection of Metals and Physical Chemistry of Surfaces*, 52(3), pp.467-474.
4. Mahato, S. and Behera, S.K., 2016. Oxidation resistance and microstructural evolution in MgO–C refractories with expanded graphite. *Ceramics International*, 42(6), pp.7611-7619.